engineering proceedings

MDPI

Proceedings Paper

Characterization of Porcine Skin Using a Portable Time-Domain Optical Coherence Tomography System †

Maria Cecilia Galvez [1,2], Jumar Cadondon [1,3,*], Paulito Mandia [1,4], Ernest Macalalad [5], Edgar Vallar [1,2] and Tatsuo Shiina [4]

1 Environment and Remote Sensing Research (EARTH) Laboratory, Department of Physics, De La Salle University, 2401 Taft Avenue, Manila 0922, Philippines; email1@email.com (M.C.G.); email2@email.com (P.M.); email3@email.com (E.V.)
2 Applied Research for Community, Health and Environment Resilience and Sustainability (ARCHERS), Center Natural Sciences and Environmental Research (CENSER), De La Salle University, 2401 Taft Avenue, Manila 0922, Philippines
3 Division of Physical Sciences and Mathematics, College of Arts and Sciences, University of the Philippines Visayas, Miagao, Iloilo, Philippines
4 Graduate School of Engineering, Chiba University, 1-33 Yayoi-cho, Inage-ku, Chiba 2638522, Japan; email4@email.com (T.S.)
5 Department of Physics, Mapua University, 658 Muralla St., Intramuros, Manila, Philippines; email4@email.com (E.M.)
* Correspondence: jgcadondon@up.edu.ph
† Presented at the 10th International Electronic Conference on Sensors and Applications (ECSA-10), 15–30 November 2023; Available online: https://ecsa-10.sciforum.net/.

Abstract: Optical Coherence Tomography (OCT) is an imaging tool to visualize the cross-section of a sample. Additionally, this device can measure the sample's physical properties. This experiment used a portable version to measure the epidermal thickness and dermal extinction coefficient of porcine skin obtained from different anatomical sites. The thinnest epidermis was found to be from the ear region, while the thickest is from the leg. Meanwhile, the lowest dermal extinction coefficient was from the ear, while the highest was from the belly. These measured properties can be used as aids for diagnosing various skin conditions in humans and animals.

Keywords: time-domain optical coherence tomography; porcine skin; extinction coefficient; skin conditions

Citation: Galvez, M.C.; Cadondon, J.; Mandia, P.; Macalalad, E.; Vallar, E.; Shiina, T. Characterization of Porcine Skin Using a Portable Time-Domain Optical Coherence Tomography System. *Eng. Proc.* **2023**, *56*, x. https://doi.org/10.3390/xxxxx

Academic Editor(s):

Published: 15 November 2023

1. Introduction

The skin is the outermost organ of the body. As such, it is the first line of defense of the organism from the environment and dehydration. Therefore, the skin needs to maintain its structural integrity to maintain homeostasis within the organism.

In an individual, skin properties can vary depending on anatomic location, age, sex, occupation, and many other factors [1,2]. The person's health condition may also alter the properties of the skin. Epidermal thickness has been used to study skin conditions. Increased epidermal thickness can be seen in patients with actinic keratosis, which is a condition that may lead to skin cancer [3]. On the other hand, decreased epidermal thickness can result from skin aging due to exposure to ultraviolet radiation [4]. Skin thickness can give a clue about the proliferation of epidermal cells; hence, it can be used to measure the degree of healing [5] and the effectiveness of drug delivery [6].

Traditionally, epidermal thickness was measured by excising a small skin region and viewing it under a light microscope [7]. While biopsy remains the gold standard in diagnostics, it is invasive and requires a significant of time for tissue processing. Newer methods of measuring epidermal thickness include high-resolution ultrasound [8] and optical

coherence tomography (OCT) [9]. Both methods are non-invasive and, hence, can be used in vivo.

Studies have also shown that the extinction coefficient (EC) of tissue changes along with chemical and structural changes of the skin during disease states. Edematous areas are due to increased water content, leading to reduced EC. Similarly, oral squamous cell carcinoma tissues showed lower extinction coefficient measurements than that of normal oral tissues [10], while pustular lesions have increased signal scattering, thus increasing the EC [11]. Due to ethical considerations and sample availability, animal tissue is the most suitable subject before testing on human volunteers, especially when using a diagnostic modality still under development.

The animal whose skin is found to have the closest resemblance to human skin regarding hair and lipid distribution, and immunogenicity is that of the pig [12,13]. Porcine skin is a possible model for studies on UV protection and epidermal morphology [14]. The wound-healing process and cell proliferation of human and porcine skin are similar [15]. It makes porcine skin the ideal candidate for our OCT study in human skin modeling. The first published OCT paper was in 1991, showing an image of the human retina [16]. OCT are vastly applied in dentistry [17], dermatology [18], and agriculture [19]. There are two types of OCT which are dependent on frequency and time. The absence of a movable reflector allows frequency domain (FD-OCT) to acquire signals faster than time domain (TD-OCT). FD-OCT is associated rapid scan speed and higher resolution in contrast to TD-OCT. It also increases signal-to-noise ratio [20,21]. However, the simple design and cheaper components make TD-OCT a viable type today [22]. It can also penetrate deeper as compared to FD-OCT. In this study, a time-domain OCT was developed.

This study aims to characterize porcine skin in terms of epidermal thickness and extinction coefficient of the dermis since these properties can easily be extracted from a single A-scan. Information derived from studies like these is useful in modeling human skin conditions, which can be later utilized for rapid, non-invasive screening and diagnosis of diseases. Furthermore, this study can also extend to veterinary medicine to benefit non-human species.

2. Materials and Methods

TD-OCT is based on the Michelson interferometer as shown in Figure 1a.

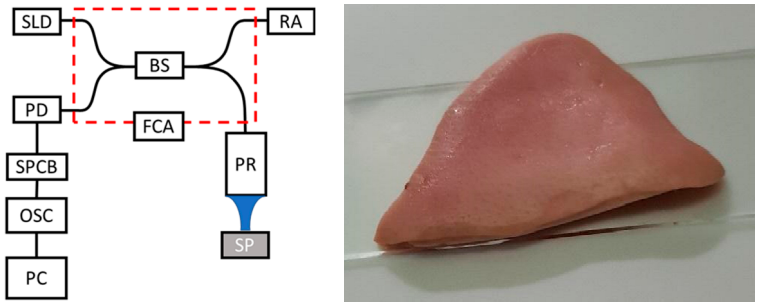

(**a**) (**b**)

Figure 1. (**a**) The schematic diagram of the TD-OCT system. Superluminescent diode (SLD); Photodiode (PD); Signal processing circuit board (SPCB); Oscilloscope (Osc); Personal computer (PC); Beam splitter (BS); Reference arm (RA); Probe (PR); Sample (SP); Fiber coupler assembly (FCA) (enclosed in red box) [23]. (**b**) Porcine skin, ear part.

The reference mirror is designed as rotating retroreflector instead of moving in translation motion [24]. The advantage of a rotating mechanism over a translational one is a more extended scanning range, which can be easily adjusted by changing the retroreflector's rotation radius. Using a rotating reflector, the repeatability has improved with an optical path difference at angles less than ±20 degrees. A 1310 nm SLD (Anritsu Co. Ltd., Kanagawa, Japan) with spectral width of 106 nm and an average axial resolution of 7 μm in air. The detailed discussion on the mechanism was discussed by Shiina et al. [24]. This

system has been used for gelatin-skin-based phantoms [23,25] and leaf structures [26]. The specifications of the TD-OCT system are summarized in Table 1.

Table 1. Specifications of the TD-OCT system [22].

Specification	Value
Center wavelength	1310 nm
Spectral width	106 nm
Axial resolution	7 μm
Lateral resolution, spot size	6 μm
Numerical aperture	0.14
Scanning rate	25 scans/s
Scanning depth in air	12–14 mm

Porcine skin was bought from a local market. Skin samples were obtained from different parts, namely the belly, buttocks, leg, cheek, and ear. A piece of skin was mounted onto a glass slide, as shown in Figure 1b. The thickness can also be measured since the entire epidermal layer can be visualized from the A-scan. Light from the probe cannot penetrate the total thickness of the dermis; hence, dermal thickness cannot be assessed. On the other hand, the epidermal extinction coefficient cannot be obtained with the current specifications of the OCT system, so the dermal extinction coefficient was measured instead. A detailed discussion on the determination of extinction coefficients is previously published by Galvez et al. (2021) [23].

3. Results and Discussion

OCT attenuation has been increasingly used for tissue analysis and characterization. For heterogeneous samples like the skin, the A-scan may contain several prominent peaks representing boundaries of various surfaces [23,25]. Figure 2 is an A-scan of porcine skin at the belly. The use of multiple A-scans presents a possible use of OCT to characterize porcine skin at different sites [27].

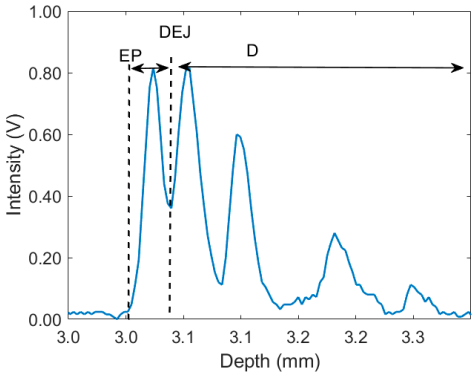

Figure 2. A-scan of porcine skin: EP, epidermis; DEJ, dermo-epidermal junction; D, dermis.

Aside from the surface peak of the epidermis, another prominent peak is the dermis's. Histologically, a very thin dermo-epidermal junction separates these two skin layers. Table 2 shows the epidermal thickness of porcine skin at various sites. It can be shown that the epidermal thickness in belly produces higher standard deviations compared to other parts. Higher errors were also observed in the belly's extinction coefficient. Larger errors are partly due to having less particles at these regions which leads to low values and slow variation of backscatter intensity. It also causes significant scattering intensity fluctuations [28,29].

Table 2. Epidermal thickness and extinction coefficient of porcine skin from various sites.

Epidermal Thickness (μm)	Belly	Leg	Buttocks	Cheek	Ear
Mean	92.38	95.22	64.64	77.72	60.13
Median	85.13	93.01	61.48	78.83	59.91
St Dev	27.30	16.64	13.18	12.03	4.70
Extinction Coefficient (1/mm)	Belly	Leg	Buttocks	Cheek	Ear
Mean	6.42	2.65	4.67	4.36	2.31
Median	6.33	2.45	3.80	3.82	2.48
St Dev	2.87	0.77	1.87	1.94	1.97

The ear epidermis was observed to be the thinnest, followed by the buttocks and cheek. These findings were consistent with other works [13,30] except for the belly, which in this research is one of the thickest compared to others. Since the epidermal layer is fragile, the data points were insufficient to compute the extinction coefficient. The high standard deviations of the values may be due to the heterogeneous nature of the skin. Another study limitation is that the skin samples were frozen for about a week before scanning.

4. Conclusions

Using OCT, epidermal thickness and dermal extinction coefficients were obtained at different pig body parts. The thinnest epidermis was found on the ear, consistent with present literature. Even without using B-scans, which require more processing time than a single A-scan. This study showed preliminary measurements and importance of A-scan in epidermal thickness. Thus, we can use OCT as a rapid, non-invasive tool as an aid for the diagnosis of skin conditions, not just in humans but also in other animals as well.

Author Contributions: Conceptualization, M.C.G.; methodology, T.S. and P.M.; software, E.M.; validation and formal analysis, M.C.G., J.C. and E.V.; investigation, P.M.; writing—original draft preparation, P.M. and J.C.; writing—review and editing, M.C.G., E.V. and T.S., J.C.; visualization, P.M. All authors have read and agreed to the published version of the manuscript.

Funding: This research was funded by the Commission on Higher Education (CHED) of the Philippine Government for the project entitled "Development of a Portable Optical Coherence Tomography System for the Evaluation of Human Skin Analogues".

Institutional Review Board Statement: Not applicable.

Informed Consent Statement: Not applicable.

Data Availability Statement: The data presented in this study are available on reasonable request from the corresponding author.

Acknowledgments: The authors are grateful for the support from the Commission on Higher Education, De La Salle University through the University Research Coordination Office (DLSU-URCO), Department of Science and Technology- ASTHRDP Program, University of the Philippines Visayas, Mapua University, and Chiba University.

Conflicts of Interest: The authors declare no conflict of interest. The funders had no role in the design of the study, in the collection, analyses, or interpretation of data; in the writing of the manuscript; or in the decision to publish the results.

References

1. Gambichler, T.; Matip, R.; Moussa, G.; Altmeyer, P.; Hoffmann, K. In Vivo Data of Epidermal Thickness Evaluated by Optical Coherence Tomography: Effects of Age, Gender, Skin Type, and Anatomic Site. *J. Dermatol. Sci.* **2006**, *44*, 145–152. https://doi.org/10.1016/j.jdermsci.2006.09.008.
2. James, W.D.; Elston, D.K.; Treat, J.R.; Rosenbach, M.A.; Neuhaus, I.M. *Andrews' Diseases of the Skin-Clinical Dermatology*, 13th ed.; Elsevier: Edinburgh, Scotland, 2020.
3. Jerjes, W.; Hamdoon, Z.; Rashed, D.; Sattar, A.A.; Hopper, C. In Vivo Optical Coherence Tomography in Assessment of Suspicious Facial Lesions: A Prospective Study. *Photodiagnosis Photodyn. Ther.* **2021**, *36*, 102493. https://doi.org/10.1016/J.PDPDT.2021.102493.
4. Olsen, J.; Gaetti, G.; Grandahl, K.; Jemec, G.B.E. Optical Coherence Tomography Quantifying Photo Aging: Skin Microvasculature Depth, Epidermal Thickness and UV Exposure. *Arch. Dermatol. Res.* **2022**, *314*, 469–476. https://doi.org/10.1007/S00403-021-02245-8.
5. Mariia, K.; Arif, M.; Shi, J.; Song, F.; Chi, Z.; Liu, C. Novel Chitosan-Ulvan Hydrogel Reinforcement by Cellulose Nanocrystals with Epidermal Growth Factor for Enhanced Wound Healing: In Vitro and in Vivo Analysis. *Int. J. Biol. Macromol.* **2021**, *183*, 435–446. https://doi.org/10.1016/J.IJBIOMAC.2021.04.156.
6. Roberts, M.S.; Cheruvu, H.S.; Mangion, S.E.; Alinaghi, A.; Benson, H.A.E.; Mohammed, Y.; Holmes, A.; van der Hoek, J.; Pastore, M.; Grice, J.E. Topical Drug Delivery: History, Percutaneous Absorption, and Product Development. *Adv. Drug Deliv. Rev.* **2021**, *177*, 113929. https://doi.org/10.1016/J.ADDR.2021.113929.
7. Therkildsen, P.; Hædersdal, M.; Lock-Andersen, J.; Olivarius, F.D.F.; Poulsen, T.; Wulf, H.C. Epidermal Thickness Measured by Light Microscopy: A Methodological Study. *Ski. Res. Technol.* **1998**, *4*, 174–179. https://doi.org/10.1111/J.1600-0846.1998.TB00106.X.
8. van Mulder, T.J.S.; de Koeijer, M.; Theeten, H.; Willems, D.; van Damme, P.; Demolder, M.; de Meyer, G.; Beyers, K.C.L.; Vankerckhoven, V. High Frequency Ultrasound to Assess Skin Thickness in Healthy Adults. *Vaccine* **2017**, *35*, 1810–1815. https://doi.org/10.1016/J.VACCINE.2016.07.039.
9. Czekalla, C.; Schönborn, K.H.; Lademann, J.; Meinke, M.C. Noninvasive Determination of Epidermal and Stratum Corneum Thickness in Vivo Using Two-Photon Microscopy and Optical Coherence Tomography: Impact of Body Area, Age, and Gender. *Skin Pharmacol. Physiol.* **2019**, *32*, 142–150. https://doi.org/10.1159/000497475.
10. Yang, Z.; Shang, J.; Liu, C.; Zhang, J.; Liang, Y. Identification of Oral Cancer in OCT Images Based on an Optical Attenuation Model. *Lasers Med. Sci.* **2020**, *35*, 1999–2007. https://doi.org/10.1007/s10103-020-03025-y.
11. Welzel, J. Optical Coherence Tomography in Dermatology: A Review. *Ski. Res. Technol.* **2001**, *7*, 1–9. https://doi.org/10.1034/j.1600-0846.2001.007001001.x.
12. Summerfield, A.; Meurens, F.; Ricklin, M.E. The Immunology of the Porcine Skin and Its Value as a Model for Human Skin. *Mol. Immunol.* **2015**, *66*, 14–21. https://doi.org/10.1016/J.MOLIMM.2014.10.023.
13. Khiao In, M.; Richardson, K.C.; Loewa, A.; Hedtrich, S.; Kaessmeyer, S.; Plendl, J. Histological and Functional Comparisons of Four Anatomical Regions of Porcine Skin with Human Abdominal Skin. *J. Vet. Med. Ser. C: Anat. Histol. Embryol.* **2019**, *48*, 207–217. https://doi.org/10.1111/ahe.12425.
14. Brożyna, A.; Wasilewska, K.; Węsierska, K.; Barbara, W.; Chwirot, B.W. Porcine Skin as a Model System for Studies of Adverse Effects of Narrow-Band UVB Pulses on Human Skin Porcine Skin as a Model System for Studies of Adverse Effects of Narrow-Band UVB Pulses on Human Skin. *J. Toxicol. Environ. Health Part A* **2009**, *72*, 789–795. https://doi.org/10.1080/15287390902800363.
15. Vlig, M.; Boekema, B.K.H.L.; Ulrich, M.M.W. Porcine Models. *Biomater. Ski. Repair Regen.* **2019**, 297–330. https://doi.org/10.1016/B978-0-08-102546-8.00010-8.
16. Huang, D.; Swanson, E.A.; Lin, C.P.; Schuman, J.S.; Stinson, W.G.; Chang, W.; Hee, M.R.; Flotte, T.; Gregory, K.; Puliafito, C.A.; et al. Optical Coherence Tomography. *Science (1979)* **1991**, *254*, 1178–1180. https://doi.org/10.1126/science.1957169.
17. Schneider, H.; Park, K.-J.; Häfer, M.; Rüger, C.; Schmalz, G.; Krause, F.; Schmidt, J.; Ziebolz, D.; Haak, R. Dental Applications of Optical Coherence Tomography (OCT) in Cariology. *Appl. Sci.* **2017**, *7*, 472. https://doi.org/10.3390/app7050472
18. Wan, B.; Ganier, C.; Du-Harpur, X.; Harun, N.; Watt, F.M.; Patalay, R.; Lynch, M.D. Applications and future directions for optical coherence tomography in dermatology. *Br. J. Dermatol.* **2020**, *184*, 1014–1022.
19. Saleah, S.-A.; Lee, S.-Y.; Wijesinghe, R.E.; Lee, J.; Seong, D.; Ravichandran, N.K.; Jung, H.-Y.; Jeon, M.; Kim, J. Optical signal intensity incorporated rice seed cultivar classification using optical coherence tomography. *Comput. Electron. Agric.* **2022**, *198*, 107014.
20. Gabriele, M.L.; Wollstein, G.; Ishikawa, H.; Kagemann, L.; Xu, J.; Folio, L.S.; Shuman, J.S. Optical Coherence Tomography: History, Current Status, and Laboratory Work. *Invest. Opthalmol. Vis. Sci.* **2011**, *52*, 2425–2436.
21. Wang, C.; Xia, X.; Tian, B.; Zhou, S. Comparison of Fourier-Domain and Time-Domain Optical Coherence Tomography in the Measurement of Thinnest Corneal Thickness in Keratoconus. *J. Ophthalmol.* **2015**, 402925.
22. Liu, P. *Optical Coherence Tomography for Material Characterization*; Nanjing University of Aeronautics and Astronautics: Nanjing, China, 2014.
23. Galvez, M.C.; Vallar, E.; Shiina, T.; Macalalad, E.; Mandia, P. Time-Domain Optical Coherence Tomography System for Determining the Extinction Coefficient and Group Refractive Index of Gelatin-based Skin Phantoms. *Sci. Technol. Indones.* **2021**, *6*, 319–327.

24. Shiina, T.; Moritani, Y.; Ito, M.; Okamura, Y. Long-Optical-Path Scanning Mechanism for Optical Coherence Tomography. *Appl. Opt.* **2003**, *42*, 3795–3799. https://doi.org/10.1364/ao.42.003795.
25. Mandia, P.F.; Vallar, E.A.; Shiina, T.; Macalalad, E.P.; Galvez, M.C.D. Time-domain optical coherence tomography and gelatin-based skin phantom as training tools for venipuncture. *J. Phys. Conf. Ser.* **2020**, *1593*, 012032.
26. Galvez, M.C.D.; de lara, R.; Mandia, P.; Vallar, E.; Macalalad, E.; Shiina, T. Leaf Structure and Attenuation Coefficients of Citrofortunella Microcarpa Leaves Using a Portbale TD-OCT System. *ECS Trans.* **2022**, *107*, 2243–2253.
27. Gong, P.; Almasian, M.; Soest, G.; de Bruin, D.M.; van Leeuwen, T.G.; Sampson, D.D.; Faber, D.J. Parametric imaging of attenuation by optical coherence tomography: review of models, methods, and clinical translation. *J. Biomed. Opt.* **2020**, *25*, 040901.
28. Yang, H.; Zheng, G.; Li, M. A Discussion of Noise in Dynamic Light Scattering for Particle Sizing. *Part. Part. Syst. Charact.* **2008**, *25*, 406–413.
29. Huang, R.; Zhang, Q.; Qi, P.; Liu, W. Concentration Measurement of Uniform Particles Based on Backscatter Sensing of Optical Fibers. *Water* **2019**, *11*, 1955. https://doi.org/10.3390/w11091955
30. Faber, D.J.; van der Meer, F.J.; Aalders, M.C.G.; van Leeuwen, T.G. Quantitative Measurement of Attenuation Coefficients of Weakly Scattering Media Using Optical Coherence Tomography. *Opt. Express* **2004**, *12*, 4353. https://doi.org/10.1364/opex.12.004353.